VALIDATING AN ISOTOPIC AGCM WITH NEW SATELLITE MEASUREMENTS OF WATER VAPOR ISOTOPOLOGUES

Kei Yoshimura[*1]
[1]Atmosphere and Ocean Research Institute, University of Tokyo
5-1-5 Kashiwanoha, Kashiwa, Chiba 2778568, Japan; Tel: +81-4-7136-4383
Email: kei@aori.u-tokyo.ac.jp

KEY WORDS: stable water isotope, satellite spectroscopy, general circulation model

ABSTRACT: We performed an intensive verification of an isotope-incorporated atmospheric general circulation model with vapor isotope observation data by two satellite sensors in preparation for data assimilation of water isotopes. A global IsoGSM simulation forced toward the reanalysis wind field, atmospheric total column data from SCIAMACHY on Envisat, and mid-tropospheric (800 to 500 hPa) data from TES on Aura were used. For the mean climatological δD of both the total atmospheric column and the mid-troposphere layer, the model reproduced their geographical variabilities quite well. There is, however, some degree of underestimation of the latitudinal gradient (higher δD in the tropics and lower δD in mid-latitudes) compared to the SCIAMACHY data, whereas there is an over-amplification of the longitudinal variation (higher δD in South America-Atlantic-Africa and lower δD in Maritime Continent) compared to the TES data. It was also found that the two satellite products have different relationships between water vapor amount and isotopic composition. Particularly, atmospheric column mean δD, which is dominated by lower tropospheric vapor, closely follows the fractionation pattern of a typical Rayleigh-type "rain-out" process, whereas in the mid-troposphere the relationship between isotopic composition and vapor amount is affected by a "mixing" process. This feature is not reproduced by the model, where the relationships between δD and the vapor are similar to each other for the atmospheric column and mid-troposphere. Comparing on a shorter time scale, it becomes clear that the data situation for future data assimilation for total column δD is most favorable for tropical and subtropical desert areas (i.e., Sahel, southern Africa, mid-eastern Asia, Gobi, Australia, and southwest US), whereas the available mid-tropospheric δD observations cover wider regions, particularly over tropical to sub-tropical oceans.

1. INTRODUCTION

Stable isotope composition ($\delta^{18}O$ and δD) in water has been used not only as proxy information for paleoclimate reconstruction [*Dansgaard et al.*, 1969], but also as a natural tracer for hydrological cycles since the 1960s [*Dansgaard*, 1964]. Largely due to the isotope effects involved in phase changes of water, geographic and temporal variations of isotope ratios emerge in water vapor and precipitation. By using the isotope information in precipitation and vapor, one can study atmospheric vapor cycling processes on various scales, such as large-scale transport and in-cloud processes. Thus, the relationship between atmospheric processes and isotope information in water vapor and precipitation has been intensively studied since *Craig and Gordon* [1965].

Recent advances in remote sensing observations of water vapor isotopes via satellites have dramatically increased the number of observed data. *Zakharov et al.* [2004] retrieved the first latitudinal climatology for total column integrated water vapor δD values using the IMG (Interferometric Monitor for Greenhouse gases sensor) sensor on ADEOS. *Worden et al.* [2006] retrieved free tropospheric water vapor δD over tropical regions with fine temporal and spatial resolution using the TES (Tropospheric Emission Spectrometer) instrument on Aura. *Payne et al.* [2007] and *Steinwagner et al.* [2007; 2010] retrieved a global stratospheric δD distribution on a monthly basis using MIPAS (the Michelson Interferometer for Passive Atmospheric Sounding) on Envisat. *Frankenberg et al.* [2009] derived atmospheric total column δD values from SCIAMACHY measurements (Scanning Imaging Absorption Spectrometer for Atmospheric Chartography) on Envisat. Although limitations still exist in terms of spatial and temporal coverage, resolution, and accuracy, these observations have engendered greater understanding of the basic distribution of water isotopologues and the physical process that drives them. It is also worthwhile to mention that remote sensing with ground-based Fourier Transform Spectroscopy sensors has provided a useful and highly interesting new dataset (e.g., *Schneider et al.* [2010]). Furthermore, in the very recent past, precise optical analyzers for in-situ HDO measurements have become available and will provide a wealth of information in the future (e.g., *Lee et al.* [2006]; *Welp et al.* [2008]).

On the other hand, isotope-incorporated atmospheric general circulation models (AGCM) initiated by *Joussaume et al.* [1984] offer a different approach to understanding isotope distribution. They combine the physical processes associated with isotope ratio changes with dynamic and moist thermodynamic processes of the atmosphere. These models simulate the time evolution of the three-dimensional structure of water vapor isotopologue distribution with explicit consideration of complex water phase changes associated with moist physical processes in the global atmosphere. Most of the models' results generally match well with the precipitation isotope observations for continental and monthly scales. For vapor isotopes however, the models are inconsistent [*Noone and Sturm*, 2010],

and an intensive comparison with observations has not been made due to the lack of sufficient data except *Schmidt et al.*, [2005].
As an advanced effort of the modeling approach, *Yoshimura et al.* [2008] (hereafter Y08) ran an isotope-AGCM applying spectral nudging toward real atmospheric dynamics using the NCEP/DOE Reanalysis (R2; *Kanamitsu et al.* [2002]) dataset. This procedure mimics an isotope data assimilation, but without any observed isotope information. The global simulation forced by reanalysis better reproduced the isotope variations in precipitation for a wide range of time scales from daily to inter-annual. This improvement by the nudging technique was confirmed by subsequent studies (e.g., *Risi et al.* [2010]).
In this paper, we validate various aspects of the Y08 isotope-AGCM historical simulation using newly published satellite δD products from SCIAMACHY [*Frankenberg et al.*, 2009] and TES [*Worden et al.*, 2007]. This is a further step towards potential data assimilation of water vapor isotopologues and the production of objective analysis fields of isotopes, which have never yet been achieved. In the next section, the model simulation and the satellite-based products are described. The third section compares the results. A summary and conclusions follow.

2. DATA AND METHOD

2.1 SCIAMACHY δD data

In *Frankenberg et al.* [2009], δD in the entire atmospheric column was measured for the first time by the SCIAMACHY grating spectrometer onboard the European research satellite Envisat. In a wavelength window ranging from 2355 to 2375 nm, simultaneous retrievals of HDO and H_2O vertical column densities are enabled. Due to the relatively high detector noise of SCIAMACHY in the short-wave infrared channel 8, the single measurement noise (1-sigma precision error) in δD is typically 40-100 ‰, depending on total water column, surface albedo and viewing geometry. This error can be significantly reduced by averaging multiple measurements, and the averaging procedure will be described below. The footprint of each measurement is 120 km by 30 km. The retrieval period for this study is 2003 through 2005, in which a total of about 1.9 million scenes are included and the measurement values of δD are systematically and arbitrarily decreased by 20 ‰ to minimize the large scale difference to the model. More details about the retrieval procedure can be found in *Frankenberg et al.* [2009]. Most noteworthy in regard to this study is the fact that SCIAMACHY measurements are performed in the short-wave infrared, thereby exhibiting sensitivity for the entire atmospheric column, including boundary layer water vapor.

2.2 TES δD data

TES on the Aura satellite is an infrared Fourier transform spectrometer that measures the spectral infrared (IR) radiances between 650 cm^{-1} and 3050cm^{-1} in limb-viewing and nadir (downward looking) modes. The observed IR radiance is imaged onto an array of 16 detectors that have a combined horizontal footprint of 5.3 km by 8.4 km in the nadir viewing mode. In the nadir view, TES estimates of atmospheric distributions provide vertical information of the more abundant tropospheric species such as H_2O, HDO, O_3, CO, and CH_4 [*Worden et al.,* 2006]. Simultaneous profiles of HDO and H_2O are obtained from TES thermal infrared radiances between 1,200 and 1,350 cm^{-1} (7400 to 8300 nm in wavelength) using maximum a posteriori optimal estimation [*Worden et al.*, 2006]. This approach allows for a precise characterization of the errors in the ratio (HDO/H_2O) and its vertical resolution. For this analysis, mean values of the isotopic composition (δD) are calculated from averages of HDO and H_2O between 550 and 800 hPa, where the estimated profiles of δD are most sensitive. This average has a typical accuracy of 10‰ in the tropics and 24‰ at the poles. Profiles of atmospheric and surface temperature, surface emissivity, effective cloud optical depth and cloud top height are also estimated from TES radiances and are used to stratify δD analysis. A bias in the established HDO spectroscopic line strengths requires a correction of 50‰ in the estimated HDO profiles and is uniform across all observations. The bias correction accounts for the a priori constraint and vertical resolution of the HDO and H_2O profile retrieval. In this study, the retrieval period is 2005 through 2007, in which a total of about 550,000 scenes are included, and the measurement values of δD are systematically and arbitrarily increased by 20 ‰ to minimize the difference to the model field over 45°S-45°N.

2.3 Isotope General Circulation Model simulation

The Isotope-incorporated Global Spectral Model (IsoGSM) was developed by Y08 and a 30-year simulation with a global spectral nudging technique [*Yoshimura and Kanamitsu*, 2008] was performed (data available at http://hydro.iis.u-tokyo.ac.jp/~kei/IsoGSM1). The spatial and temporal resolution of the IsoGSM simulation atmospheric output is 2.5°x2.5° and 6 hourly. In this study, this nudged simulation data is used for comparisons with the satellite measurements. In this method, the large scale dynamical forcing was taken from NCEP/DOE Reanalysis 2 [*Kanamitsu et al.*, 2002], and water isotopologues were fully predicted, including their sources and sinks, without utilizing any water isotope observations. Several validation studies of this model product against limited observations

showed that the analysis is sufficiently accurate for various process studies (e.g., *Uemura et al.* [2008]; *Abe et al.* [2009]; *Schneider et al.* [2010]; *Berkelhammer et al.* [2010]).
We prepare a further experiment to examine the sensitivity of the results to the "equilibrium fraction ε," which is the degree to which falling rain droplet equilibrates with the surroundings. This parameter is very important to the isotopic exchange between falling droplet and ambient vapor (*Hoffmann et al.* [1998]; *Lee and Fung* [2008]; *Yoshimura et al.* [2010]). It is the essential reason precipitation isotopes only reflect the near surface vapor even though the condensation takes place at a much higher atmospheric level. The experiment using the smaller equilibrium fraction of 10% for convective precipitation is called E10 hereafter, whereas the control run (CTL) used an equilibrium fraction of 45%. This decrease of the parameter indicates that a rain drop in a convective cell would less isotopically interact with the ambient vapor than previously thought. The simulation period of E10 with the same nudging scheme starts from 2000, so that the impact of the initial state is sufficiently dissolved for the analysis period of 2003-2007.

2.4 Processing of the Data

From the IsoGSM simulation results, the nearest location and time of each satellite measurement are extracted for both SCIAMACHY and TES data (hereafter the process is called "collocation"). Thus we disregard the representativeness difference between the model and the data. The extraction process for SCIAMACHY data is different from that for TES. Since a single measurement by SCIAMACHY has a larger random error [*Frankenberg et al.* 2009], we average multiple measurements that have been collected for a grid of 2.5°x2.5° in 6 hours, whereas no averaging of multiple measurements is taken into account for the TES-IsoGSM collocation. We set the threshold value for the averaging as 10. Therefore, the average of the SCIAMACHY measurements is only considered for comparison with IsoGSM if the measurements were made more than 10 times inside a cell of 2.5°x2.5° for 6 hours. After this procedure, the amount of comparable data shrinks to about 50000, mainly covering the desert regions because of the high IR reflectivity and absence of clouds there [*Frankenberg et al.* 2009].
Even though there is some degree of vertical sensitivity regarding the averaging kernels (AK) of the satellite sensors' retrieval algorithms [*Lee et al.*, 2010], we have simply extracted the mean δD values in the vapor contents of the total atmospheric column and the 800-500 hPa level for SCIAMACHY and TES, respectively. The TES's AK vary in time and space and TES is less sensitive where there is little water vapor, such as at high latitudes. With the low sensitivity, the retrieval results tend to be close to the a priori assumption, which is why TES sees a smaller latitudinal gradient and smaller seasonal cycles at high latitudes [*Worden et al.*, 2006]. On the other hand, SCIAMACHY's AK do not vary in time and space. Also for TES, the real atmospheric temporal variations of δD in vapor are much larger than the systematic impact of TES's AK. Therefore, assigning the correct time and space for comparison is likely much more important than this bias. Thus, the use of the nudged simulation is essential for this study.

3. RESULTS

3.1 Comparison of annual and seasonal climatology

In Figure 1, the annual mean climatology of the SCIAMACHY measurement (Fig.1a) and the collocated IsoGSM simulations (Fig.1b and 1d) are shown. IsoGSM is a state-of-the art model that captures the general two-dimensional isotope distribution well. The common maxima over central Africa and the Amazon are likely due to the impact of evapotranspiration from the land surface, leading to isotope enrichment. Over these regions, the "continental effect" is weaker than over mid- and high latitudes as shown in *Frankenberg et al.* [2009]. It is important to note that the annual averages shown in these figures are biased towards specific seasons because the observation frequency depends on many factors, such as minimum signal-to-noise-ratio, cloud cover, or thresholds on solar zenith angles (resulting in less measurement at high latitudes where snow cover and high solar angles reduce the signal level in the short-wave-infrared). Whereas this must be taken into account when interpreting the data, it does not affect the model-data comparison because of the collocation.
Despite the qualitatively good agreement, there are also some discrepancies, and the most obvious difference is that the simulated latitudinal isotope gradient is smaller than in the observations. These differences between the model and SCIAMACHY observations are shown in Figure 1c and 1e and they reveal that compared to SCIAMACHY, both experiments in IsoGSM underestimate the tropical δD values whereas they overestimate sub-tropical δD. The difference between the two experiments (Figure 1b and 1d) is relatively smaller, indicating that the impact of the equilibrium fraction factor ε is not as sensitive as at the atmospheric column (will be shown in Figure 2).
In Figure 2, the geographical comparisons between the TES data and the collocated IsoGSM results are shown in a similar manner. As for the SCIAMACHY results, the spatial pattern is qualitatively well simulated by both experiments (Fig.2a, 2b, and 2d). However, the model now overestimates the latitudinal gradient, in contrast to the comparison with SCIAMACHY. This might be partly because the TES sensitivity declines at increasing latitudes so that the retrieved values become closer to the a priori, in turn damping both the seasonality and the latitudinal

gradients. Moreover, there are large underestimations over the Maritime Continent and Central America as illustrated in Figure 2c, where convective precipitation is most significant. The reason for this big discrepancy will be discussed below.

In Figure 2d and 2e, we compare the E10 results with the satellite retrievals. The impact of changing the equilibrium fraction is apparent over the Maritime region where the discrepancy in the control run was large. The large change in the mid-tropospheric vapor isotope ratio is compensated by the changes in precipitation (figure not shown) and surface vapor isotope ratios (difference between Figure 1b and 1d) due to the mass balance, but the compensated changes are smaller because of the larger amount of water at near surface or in precipitation than at mid-troposphere.

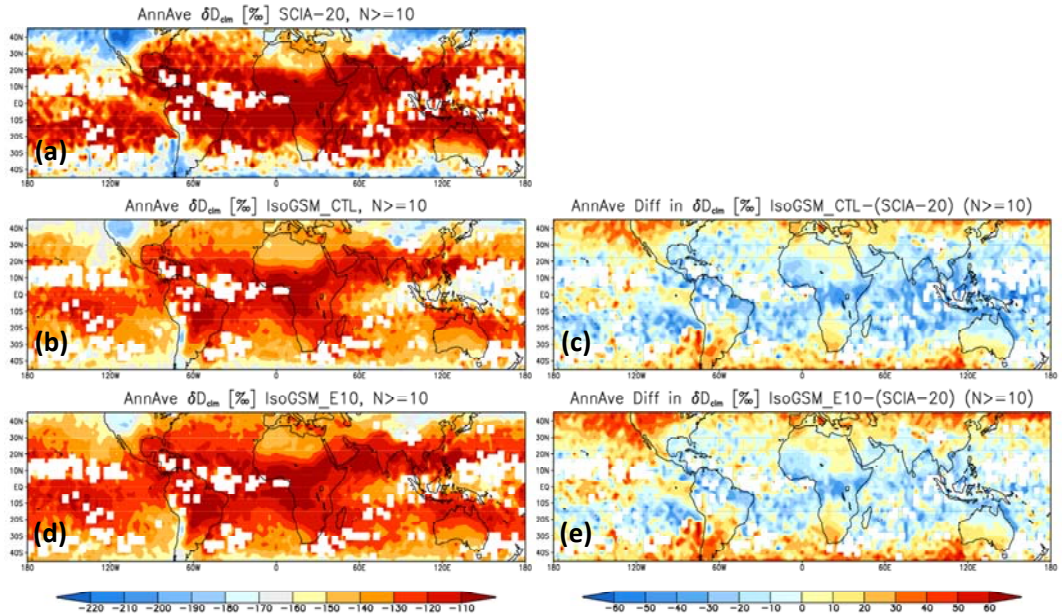

Figure 1: Left column; annual mean climatology of δD in atmospheric vapor for SCIAMACHY (a), collocated IsoGSM CTL experiment (b), and collocated IsoGSM E10 experiment (d). Right column; difference between the satellite measurements and model simulations for CTL (c) and E10 (e). SCIAMACHY δD data is systematically decreased by 20 ‰.

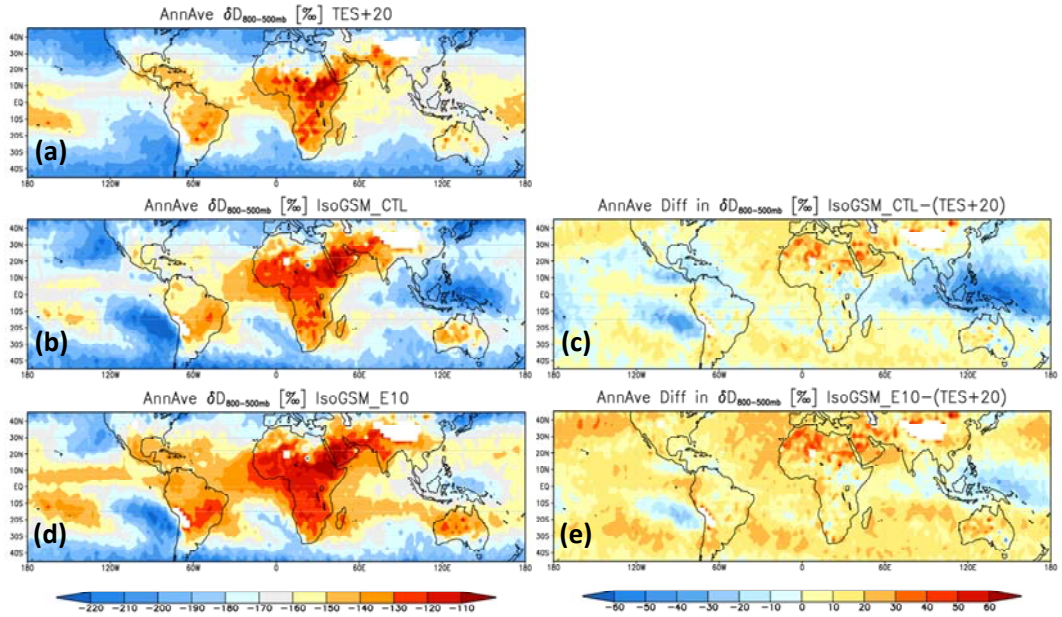

Figure 2: Same as Figure 1, but for TES mid-tropospheric (800 to 500 hPa pressure) observation. TES δD data is systematically increased by 20 ‰.

3.2 Relationship between vapor amount and δD

Figure 3 presents relationships between water vapor amount (volume mixing ratio or VMR in ‰v) and its δD in the satellite observations and the simulation over tropical to mid-latitudinal regions (45°S to 45°N). Both axes are in logarithm representation; i.e., the vertical axis is log(δD+1), and the horizontal axis is log of VMR, so that a typical

Rayleigh distillation process should form a straight line whose slope equals the fractionation factor α minus 1. Figure 3a to 3c, in which both the SCIAMACHY (blue dots) and TES observations (red dots) are plotted, indicates that the slopes of the linear regressions in SCIAMACHY are steeper than those of TES. However, these slopes (0.056~0.068 for SCIAMACHY and 0.025~0.043 for TES) are all smaller than that of a typical Rayleigh distillation process line (black solid lines), which should be around 0.08 (Majoube, 1971a, 1971b). This difference is partly caused by the omission of high latitude regions in both observational datasets, where typically Rayleigh processes dominantly affect the variation of δD. More importantly, the distinct differences between the SCIAMACHY and TES plots imply that surface vapor is more influenced by the Rayleigh-type rainout process, whereas the mid-troposphere vapor is more influenced by mixing of isotopically distinct vapor masses without isotope fractionation. Furthermore, there is a negative correlation in the TES plots where VMR is larger than 10‰v. This is due to the "amount effect" over the tropics, where much rain and its vapor are associated with some heavy isotope depletion.

In the model (Figure 3d to 3f), these relationships are differently simulated. First, the negative correlations at high vapor amounts are much more apparent than in the measurements. This feature is particularly distinguishable over the Maritime Continents and it is arguably stated that the amount effect associated with convective process is to some extent overestimated in the model. Second, the slopes of the linear regression lines for atmospheric column vapor (0.011~0.037) are slightly less inclined than those for mid-troposphere (0.030~0.051), whereas the satellite observations showed the opposite. Third, these simulated values for the SCIAMACHY observation have much shallower slopes than the observation, whereas both of the slopes are more similar for TES.

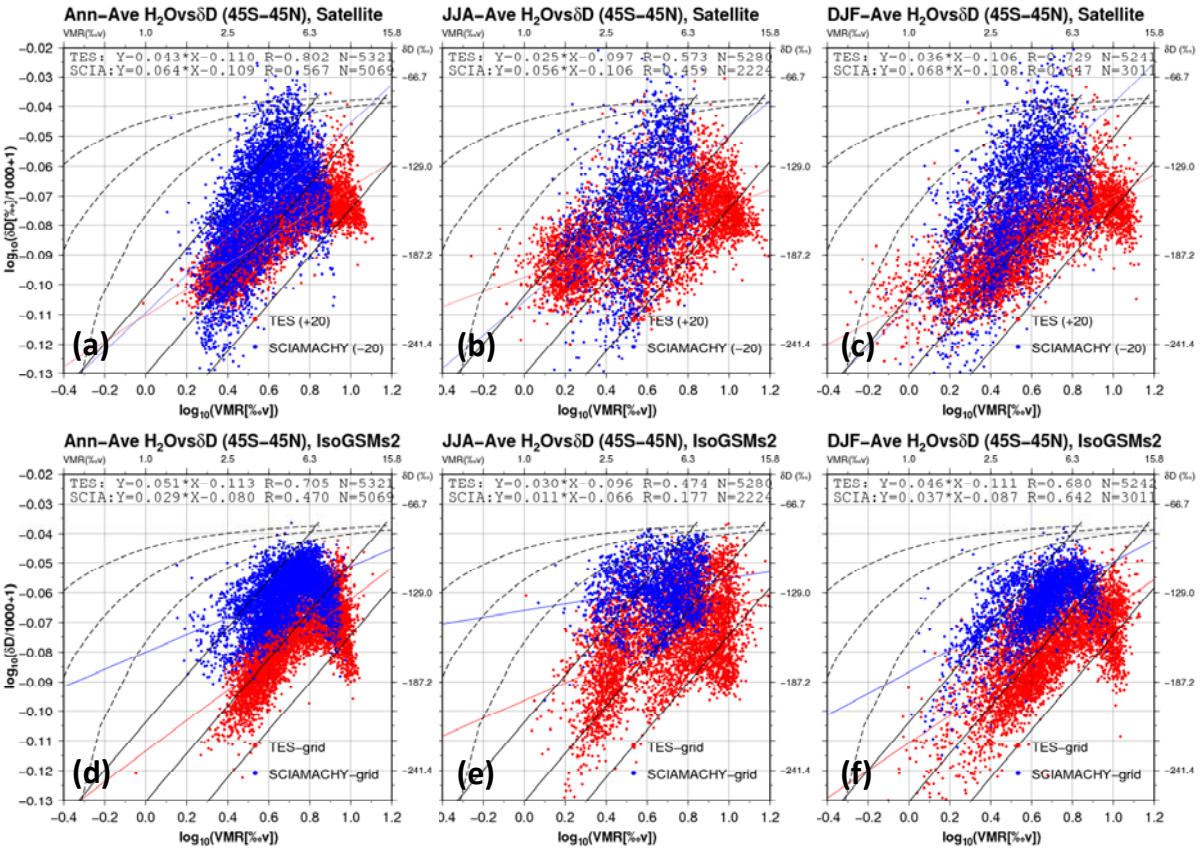

Figure 3: Scatter diagrams between vapor δD and humidity in bi-logarithm expression. (a) to (c) use the satellite observation climatology, and (d) to (f) use IsoGSM E10 simulation climatology. Blue and red dots represent SCIAMACHY and TES observations (or collocations), respectively. (a) and (d) are for annual average, (b) and (e) are for JJA, (c) and (f) are for DJF. The black solid lines indicate the Rayleigh-type fractionation, where heavy isotopes are preferably removed from vapor by condensation, starting from three typical vapors originating from the sea with 5°C, 15°C, and 25°C. The black dashed lines indicate so-called "mixing lines", which represent the mixing of two isotopically distinctive air masses.

3.3 Comparison in short-term temporal variations

In Figure 4, the time series of atmospheric column mean δD and TPW (total precipitable water) from SCIAMACHY and the IsoGSM E10 experiment at a specific grid point of 15E and 20N (Sahel region) for the year of 2005 are shown. Since the basic feature is almost the same, the CTL experiment is omitted. As already noted, a

single gridded data point from SCIAMACHY is an average of more than 10 single measurements in a 2.5°x2.5° and 6-hour space. Single measurements by SCIAMACHY fluctuate greatly, particularly for δD, as shown by small dots in the figure. However, despite the large range of the fluctuation, the spatio-temporal averages for the vapor isotope ratio (δD) are reasonably well reproduced by the model (R=0.749). Although it may be necessary to more carefully investigate the systematic and representativeness error characteristics, the good match in variability and sufficient number of valid measurements (N=64) point to promising potential for four-dimensional data assimilation in the future.

Compared to the isotope information, the TPW from the model and measurements match much better (R=0.882), with smaller fluctuations from each dataset. Though related via Rayleigh processes, the isotopic composition has independent variability from that of water vapor amount. Consequently the assimilation of the isotope information would give some additional constraint to the model, which may affect the quality of the hydrological cycle and forecasting predictability.

Figure 5 shows similar plots to Figure 4, but for TES at 67.5E and 25N (over the Arabian Sea) for 2005. δD (Figure 5a) and volume mixing ratio of water vapor (Figure 5b) of mean middle (800 hPa to 500 hPa) tropospheric air are shown. Unlike the SCIAMACHY case, there is no spatio-temporal averaging, so that each red dot in the figure represents a single measurement by TES. Though the correlation coefficient is smaller than that of the previous figure for a SCIAMACHY time series, it is a positive correlation between observed and modeled mid-tropospheric δD (R=0.588). The amplitude of model variability is much larger than that of TES even though the TES data does not have any averaging in a grid. This means that compared to the model the TES observations appear to miss much of the short-term variability, which could be a significant limitation when data assimilation is considered. The volume mixing ratio and temperature have much higher reproducibility than δD, similar to SCIAMACHY.

Figure 6 shows two-dimensional maps of correlation coefficients obtained from the comparison of high frequency seasonal variations as in Figures 4 and 5 between SCIAMACHY and the IsoGSM E10 model run (Figure 6a and 6b), and between TES and IsoGSM E10 (Figure 6c and 6d). From the SCIAMACHY figures, it is shown that a valid grid with more than 10 comparable data during 2005 is preferably located in the tropical and subtropical desert areas (i.e, Sahel, southern Africa, middle east Asia, Gobi, Australia, and southwest US). The temporal variability of atmospheric column δD is reasonably reproduced (R > 0.6) by the model in these areas (Figure 6a). However, there are also regions of significant mismatch along the east African coast and in South Africa. The correlation coefficients of the TPW are always very high (close to 1) in all areas where data are available (Figure 6b).

TES data covers wider regions, particularly over oceans (Figure 6c and 6d). The correlation coefficients for δD vary for different locations. They have rather low values over the tropics, but higher values towards higher latitude (poleward of 20°). The same figures for humidity and temperature (not shown) show generally much larger correlation coefficients, but a similar tendency of low correlations in the inner tropics is observable. This is due to the generally small seasonality in these tropical bands.

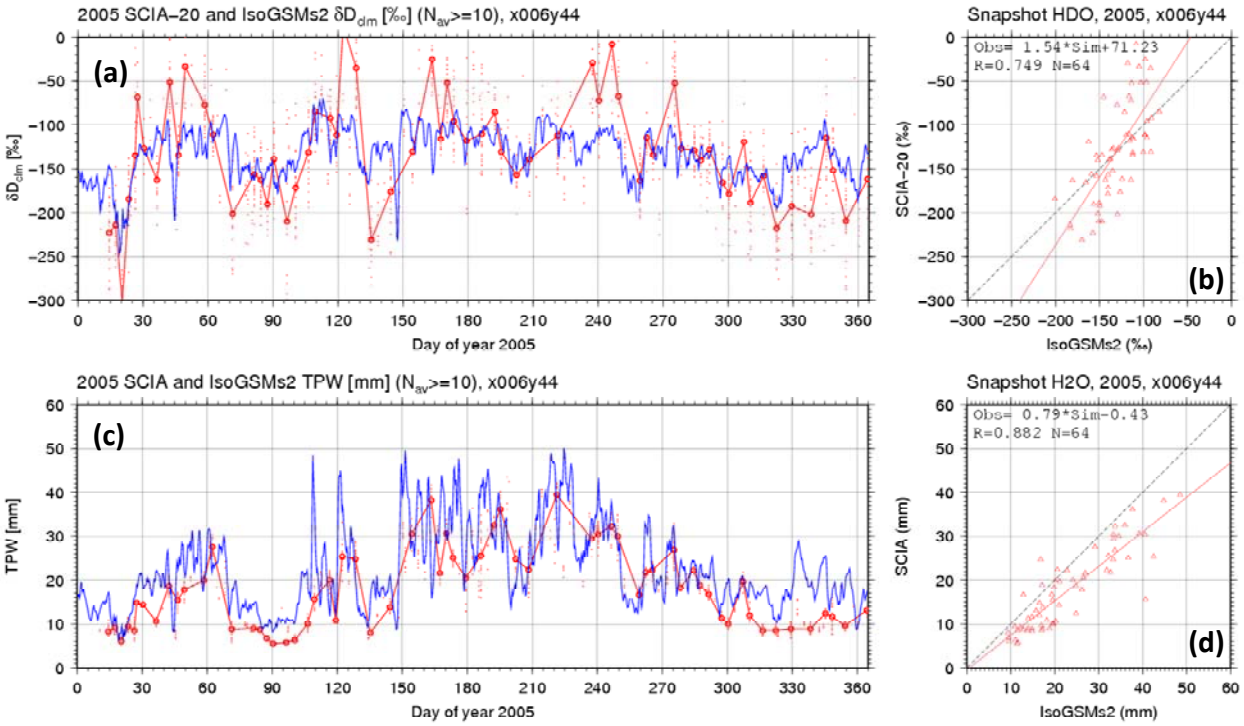

Figure 4: Comparison of the snapshot measurements with the simulation at a grid of 15°E and 20°N. δD of atmospheric column vapor is shown at the top (a and b), and the amount of total precipitable water (TPW) is shown at the bottom (c and d). Time series are on the left (a and c), and scatter plots are on the right (b and d). In the left-hand panels, red circles and blue lines represent SCIAMACHY and the IsoGSM E10 simulation, respectively, while the small red dots are from SCIAMACHY single measurements before averaging for 6-hour and 2.5°x2.5° space.

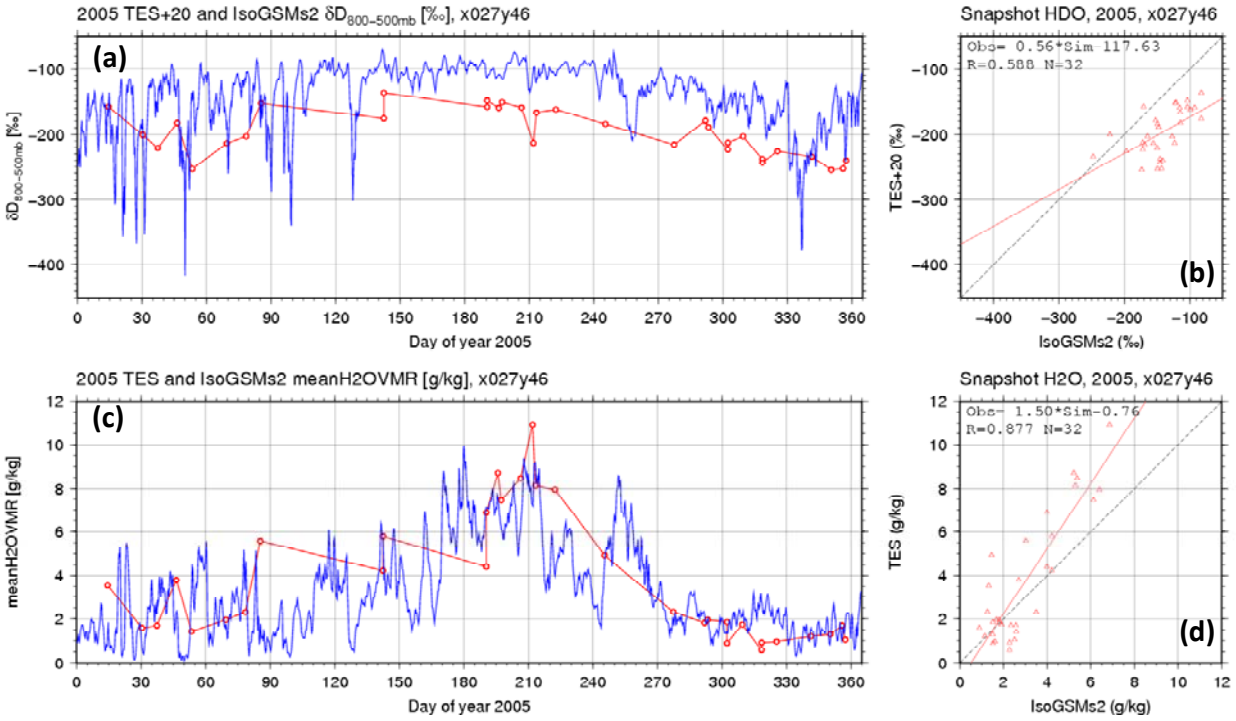

Figure 5: Similar to Figure 4, but for TES data at 67.5°E and 25°N, and for δD (a and b) and vapor volume mixing ratio (c and d) of mid-tropospheric air. Unlike Figure 4, there is no small red dot and each red circle represents a single measurement by TES.

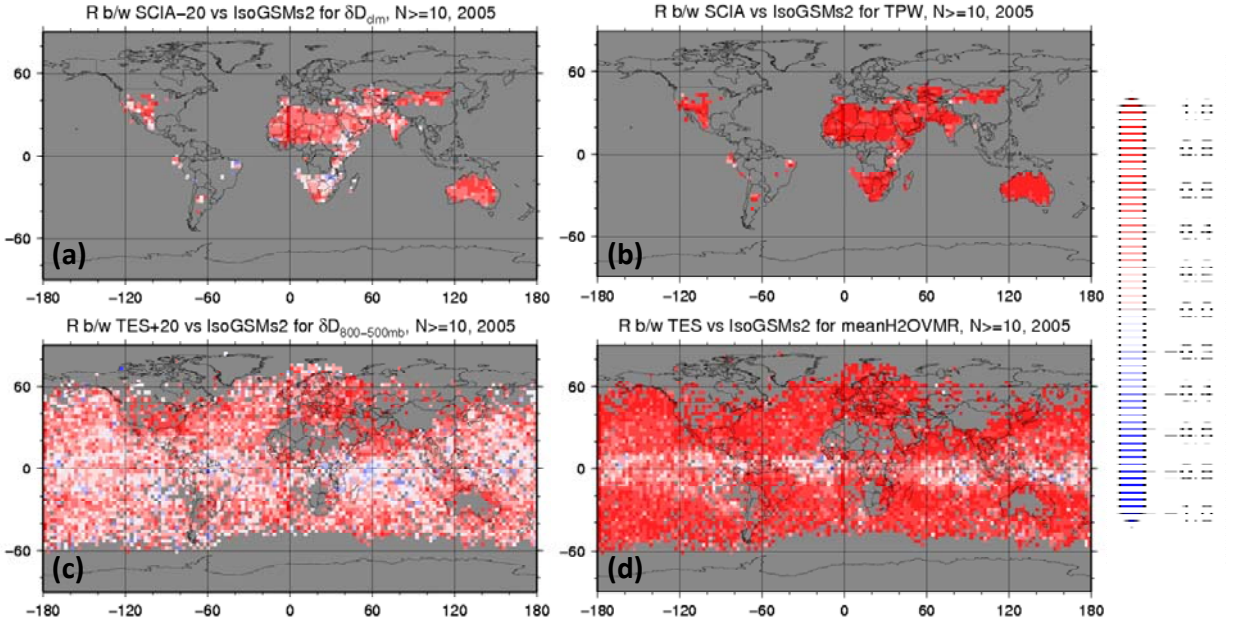

Figure 6: Global distribution maps of correlation coefficients between the time series of the SCIAMACHY or TES observations and the IsoGSM E10 simulation; (a) SCIAMACHY atmospheric column δD, (b) SCIAMACHY total precipitable water, (c) TES mid-tropospheric δD, and (d) TES mid-tropospheric volume mixing ratio.

4. SUMMARY AND CONCLUSIONS

In preparation for data assimilation of water isotopes, we have performed an intensive verification of an isotope-incorporated AGCM with vapor isotope observation data by two satellite sensors. A global IsoGSM simulation forced toward the reanalysis dynamical field, atmospheric column data from SCIAMACHY on Envisat, and mid-tropospheric (800 to 500 hPa) data from TES on Aura were used. The model reproduced the geographical variability of the mean climatological δD of the total atmospheric column and of the mid-troposphere quite well. There is, however, a clear underestimation of the latitudinal gradient (higher δD in the tropics and lower δD in mid-latitudes) compared to the SCIAMACHY data, whereas there is an over-amplification of the longitudinal variation (higher δD over South America-Atlantic-Africa and lower δD over the Maritime Continent) compared to the TES data.

It was found that the two satellite products have different relationships between the water vapor amount and its isotopic composition. In many ways, both satellite products are complementary (SCIAMACHY samples total column and is best over the continents whereas TES measures between 500-800hPa and is most reliable over oceans). Particularly, atmospheric column mean δD, which is dominated by lower tropospheric vapor, exhibits a closer relationship with a typical Rayleigh-type "rain-out" process with isotopic fractionation, whereas in the mid-troposphere it is more affected by a "mixing" process. This feature is not quite reproduced by the model, where the relationships between δD and the vapor are similar to each other for both the atmospheric column and the mid-troposphere, i.e., both are mainly driven by the Rayleigh-type “rain-out” process. The seasonal variations of the vapor δD were generally adequately reproduced by the model, with some exceptions in particular regions. These regions include mid-latitudes in the Southern Hemisphere for atmospheric column δD and the Maritime Continent (20°S-20°N and 90°E-180°) for mid-tropospheric δD. The discrepancy over the Maritime Continent is likely derived from the poor representation of the isotopic behavior in convective processes, and it was slightly improved in the model run where the equilibrium fraction was reduced, which restrains the isotopic exchange between falling droplets and ambient vapor.

Finally, we compared the model and the satellite data on a shorter time scale. We found that for total column δD, SCIAMACHY measurements show larger fluctuations than the model, but both datasets correlate reasonably well. On the contrary for mid-tropospheric δD, the model’s short-term fluctuation range is larger in the mode than for TES measurement. It is clear that the data situation for future data assimilation is best for tropical and subtropical desert areas (i.e, Sahel, southern Africa, middle eastern Asia, Gobi, Australia, and southwestern US) for total column δD, whereas the available mid-tropospheric δD observations cover wider regions, particularly over oceans.

This paper compared two satellite products and a model simulation on various scales in time and space. Some of the discrepancies between the model and the observations found in this study could be corrected when performing data assimilation, which may lead to significant improvement of four-dimensional analyses of water isotope distribution, which in turn would provide us with information to investigate further details of atmospheric hydrologic cycles.

References:

Abe, O., S. Agata, M. Morimoto, M. Abe, K. Yoshimura, T. Hiyama, and N. Yoshida, 2009: A 6.5-year continuous record of sea surface salinity and seawater isotopic composition at Harbor of Ishigaki Island, southwest Japan, *Isotopes in Environmental and Health Studies*, **45**, 247-258.

Bekelhammer, M., L. Stott, K. Yoshimura, K. Johnson, and A. Sinha, 2010: Synoptic and mesoscale controls on the isotopic composition of precipitation in the southwestern US, submitted to *Clim. Dyn*.

Craig, H. and L. Gordon, 1965: Deuterium and oxygen-18 variations in the ocean and the marine atmosphere. In Stable Isotopes in Oceanographic Studies and Paleotemperatures (ed. E. Tongiorgi), Spoleto, Italy, 9–130.

Dansgaard, W., 1964: Stable isotopes in precipitation. *Tellus*, **16**, 436-468.

Dansgaard, W., S. J. Johnsen, J. Møller and C. C. Langway, Jr. 1969: One thousand centuries of climatic record from camp century on the Greenland ice sheet, *Science*, **166**, 377-380.

Frankenberg, C., K. Yoshimura, T. Warneke, I. Aben, A. Butz, N. Deutscher, D. Griffith, F. Hase, J. Notholt, M. Schneider, H. Schrijver, and T. Röckmann, 2009: Dynamic processes governing the isotopic composition of water vapor as observed from space and ground, *Science*, **325**, 1374-1377, doi: 10.1126/science.1173791.

Joussaume, S., R. Sadourny, and J. Jouzel, 1984: A general circulation model of water isotope cycles in the atmosphere, *Nature*, **311**, 24– 29.

Kanamitsu, M., W. Ebisuzaki, J. Woolen, J. Potter, and M. Fiorino, 2002: NCEP/DOE AMIP-II Reanalysis (R-2), *Bull. Amer. Meteor. Soc.*, **83**, 1631-1643.

Lee, J., J. Worden, D. Noone, K. Bowman, A. Eldering, A. Legrande, J.-L. F. Li, G. Schmidt, and H. Sodemann, 2010: Relating tropical ocean clouds to moist processes using water vapor isotope measurements, *Atmos. Chem. Phys. Discuss.*, **10**, 17407-17434.

Lee, J. -E. and I. Fung, 2008: "Amount effect" of water isotopes and quantitative analysis of post-condensation processes, *Hydrol. Process.*, **22**, 1-8.

Lee, X., R. Smith, and J. Williams, 2006: Water vapor 18O/16O isotope ratio in surface air in New England, USA. *Tellus*, **58B**, 293–304.

Noone, D., and C. Sturm, 2010: Comprehensive dynamical models of global and regional water isotope distributions. In: *West, J., G. Bowen, T. Dawson and K. Tu (eds.) Isoscapes*, Springer, 195-219.

Payne, V. H., D. Noone, A. Dudhia, C. Piccolo, and R. G. Grainger, 2007: Global satellite measurements of HDO and implications for understanding the transport of water vapour into the stratosphere, *Q. J. R. Meteorol. Soc.*, **133**, 1459-1471.
Risi, C., S. Bony, F. Vimeux and J. Jouzel, 2010: Water stable isotopes in the LMDZ4 General Circulation Model: model evaluation for present day and past climates and applications to climatic interpretation of tropical isotopic records, *J. Geophys. Res.*, **115**, doi:10.1029/2009JD013255.
Schmidt, G. A., G. Hoffmann, D. T. Shindell, and Y. Hu, 2005: Modeling atmospheric stable water isotopes and the potential for constraining cloud processes and stratosphere-troposphere water exchange, *J. Geophys. Res.*, **110**, D21314, doi:10. 1029/2005JD005790.
Schneider, M., K. Yoshimura, F. Hase, and T. Blumenstock, 2010: The ground-based FTIR network's potential for investigating the atmospheric water cycle, *Atmos. Chem. Phys.*, **10**, 3427-3442.
Steinwagner, J., M. Milz, T. von Clarmann, N. Glatthor, U. Grabowski, M. Höpfner, G. P. Stiller, and T. Röckmann, 2007: HDO measurement with MIPAS, *Atmos. Chem Phys.*, **7**, 2601-2615.
Steinwagner, J., S. Fueglistaler, G. Stiller, T. von Clarmann, M. Kiefer, P. P. Borsboom, A. van Delden and T. Röckmann, 2010: Tropical dehydration processes constrained by the seasonality of stratospheric deuterated water, *Nature Geosci.*, **3**, 262-266.
Uemura, R., Y. Matsui, K. Yoshimura, H. Motoyama, N. Yoshida, 2008: Evidence of deuterium excess in water vapour as an indicator of ocean surface conditions, *J. Geophys. Res.*, **113**, doi:1029.10/2008JD010209.
Welp, L. R., X, Lee, K. Kim, T. J. Griffis, K. A. Billmark, and J. M. Baker, 2008: $\delta^{18}O$ of water vapour, evapotranspiration and the sites of leaf water evaporation in a soybean canopy, *Plant, Cell & Environment*, **31**, doi: 10.1111/j.1365-3040.2008.01826.x.
Worden, J., *et al.* 2006: Tropospheric Emission Spectrometer observations of the tropospheric HDO/H2O ratio: Estimation approach and characterization, *J. Geophys. Res.*, **111**, D16309, doi:10.1029/2005JD006606.
Worden, J, D. Noone, and K. Bowman, 2007: Importance of rain evaporation and continental convection in the tropical water cycle, *Nature*, **445**, doi:10.1038/ nature05508
Yoshimura, K., M. Kanamitsu, D. Noone, and T. Oki, 2008: Historical isotope simulation using Reanalysis atmospheric data, *J. Geophys. Res.*, **113**, D19108, doi:1029.10/2008JD010074.
Yoshimura, K., and M. Kanamitsu, 2008: Dynamical global downscaling of global reanalysis, *Mon. Wea. Rev.*, **136**, 2983–2998.
Yoshimura, K., M. Kanamitsu, and M. Dettinger, 2010: Regional downscaling for stable water isotopes: A case study of an Atmospheric River event, *J. Geophys. Res.*, **115**, doi:10.1029/2010JD014032.
Zakharov, V. I., R. Imasu, K. G. Gribanov, G. Hoffmann, and J. Jouzel, 2004: Latitudinal distribution of the deuterium to hydrogen ratio in the atmosphere water vapor retrieved from IMG/ADEOS data, *Geophys. Res. Let.*, **31**, L12104, doi:10.1029/2004GL019433.